Time-Resolved Study of the Martensitic Phase Transition in Syndiotactic Polypropylene

Finizia Auriemma* and Claudio De Rosa

Dipartimento di Chimica, Università di Napoli "Federico II", Complesso Monte S. Angelo, Via Cintia, 80126 Napoli, Italy

Received July 24, 2003; Revised Manuscript Received September 27, 2003

ABSTRACT: The structural transformations occurring in fibers of syndiotactic polypropylene (sPP) during stretching have been studied by wide-angle X-ray diffraction measurements, using syncrotron radiation. sPP samples were cyclically stretched and relaxed at controlled rate, while recording X-ray fiber diffraction patterns and stress−strain curves. Clear evidences that the polymorphic transition between the helical form II and the trans-planar form III of sPP is a fast process and occurs on the same time scale as the rate the material is stretched, are provided. The transition of form II into form III starts during the stretching in correspondence to critical values of the stress−strain parameters. As the strain increases, crystals of form II transform into form III and the inverse transition occurs, releasing the tension. Below a critical strain, the sample is almost completely in the helical form, as in the initial unstrained state. A complete recovery of the initial dimensions of the specimen is observed, upon releasing the tension. Moreover, the total amount of crystallinity does not change during cyclic elengation and recovery. This suggests that the reversible phase transition between form II and form III does not involve the formation of any disordered, intermediate phase, i.e., it is a direct and cooperative process, implying conformational and structural rearrangements of large bundles of close neighboring chains and occurs instantaneously. These data indicate that while the driving force leading the conventional elastomers to recover the initial dimensions is merely entropic, in the case of sPP elasticity is also assisted by the enthalpic gain achieved when the sample is relaxed. When the tension is removed, both the enthalpic factor, due to the structural transition in the crystalline region, and an entropic factor, due to the conformational transition of the chains in the entangled amorphous phase, contribute to the elastic recovery of the fiber. A possible mechanism for the martensitic crystal−crystal phase transition of sPP is suggested.

Introduction

The recent discovery that C_s symmetric metallocene complexes including metals of the fourth column are able to polymerize propylene to a highly stereoregular syndiotactic polymer with high molecular weight and without regioirregularities,[1] has refocused the interest for syndiotactic polypropylene (sPP).[2−6] Samples of sPP previously obtained with vanadium based Ziegler−Natta catalysts,[7−10] showed low degrees of crystallinity and poor mechanical properties because of the high content of regio- and stereodefects.[11,12] Recent studies have pointed out that the novel sPP is highly crystalline and shows high melting temperatures and interesting mechanical properties.[5]

The polymorphic behavior of sPP has been studied in detail and several aspects related to structure-properties relationships have been clarified. Four crystalline forms, shown in Figure 1, have been described, so far. The most stable form I (Figure 1A) and the metastable form II (Figure 1B) are characterized by chains in s(2/1)2 helical conformation, packed in orthorhombic unit cells.[2,10,15]

Form I is obtained under the most common conditions of crystallization (i.e., from the melt and from solution as powder[5,13,14] or single crystals[2−4]); in the limit ordered model, right- and left-handed helices alternate along both axes of the unit cell,[2] whereas disorder in this alternation is present in samples crystallized at low temperatures.[2−4,14] Form II is less stable and is characterized by a *C*-centered structure, where 2-fold helical chains having the same chirality are included in the unit cell (Figure 1B).[15,16] The two metastable modifications, form III[17,18] (Figure 1C) and form IV[19,20] (Figure 1D), present chains in trans-planar and $(T_6G_2T_2G_2)_n$ helical conformations, respectively, and can be obtained only in oriented fibers.

Recent studies[21−23] have pointed out that sPP shows good elastic properties in a deformation range well beyond the normal elastic deformation range of all thermoplastic polymers,[24] despite the high degree of crystallinity. The outstanding mechanical properties of sPP are in contrast with the high values of the elastic modulus (≈300 MPa) and the glass transition temperature (≈0 °C), which are both much higher than those of conventional thermoplastic elastomers.[25]

In particular, it has been shown that unoriented compression-molded films of sPP behave like a typical highly crystalline material showing a plastic deformation upon stretching at room temperature.[23] The crystalline domains of form I, with chains in helical conformation, tend to assume a preferred orientation along the stretching direction originating a plastic deformation. High orientation of the crystalline phase is generally achieved. Along with this irreversible plastic deformation, a phase transition from the most stable helical form I into the metastable form III with chains in the trans-planar conformation occurs.[5] After the tension is released, the crystalline domains remain nearly oriented with the *c* axis parallel to the preferred (stretching) direction, and the trans-planar form III transforms into the more stable isochiral helical form II.[16,23] For not previously oriented material, a partial recovery of the macroscopic dimensions of the sample is obtained. Therefore, unoriented samples show only fair or poor elastic properties.[23]

* Corresponding author. Telephone: ++39 081 674341. Fax: ++39 081 674090. E-mail: auriemma@chemistry.unina.it.

10.1021/ma0350718 CCC: $25.00
Published on Web 11/20/2003

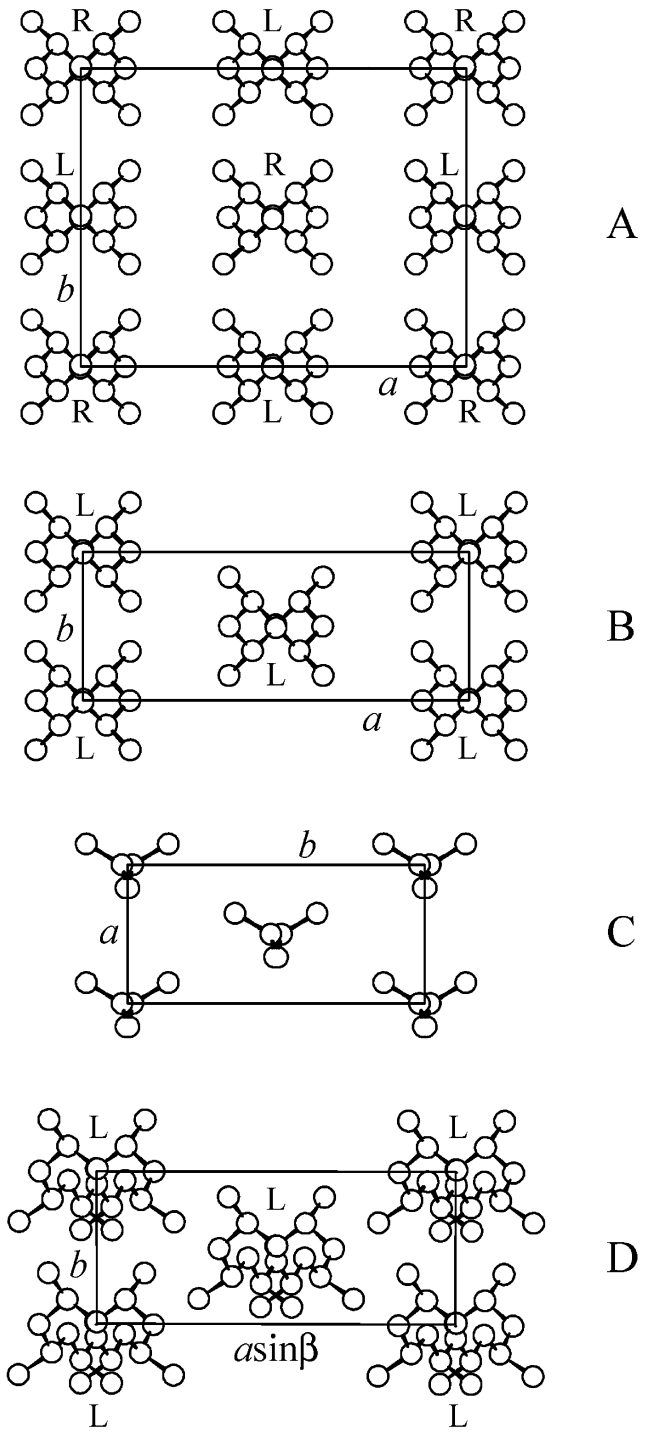

Figure 1. Models of packing of the limit ordered form I (a = 14.5 Å, b = 11.2 Å, c = 7.4 Å)[2] (A); form II (a = 14.5 Å, b = 5.6 Å, c = 7.4 Å)[15] (B); form III (a = 5.22 Å, b = 11.17 Å, c = 5.06 Å)[18] (C); form IV (a = 14.17 Å, b = 5.72 Å, c = 11.6 Å, β = 108.8°)[20] (D) of sPP. R = right-handed helix; L = left-handed helix.

Stress-relaxed fibers show, instead, very good elastic behavior upon cyclically stretching and relaxing the samples. Elasticity of sPP fibers is also associated with the reversible crystal−crystal phase transition between form II and form III.[22,23] The helical form II transforms by stretching into the metastable form III, which transforms again into the more stable helical form II by releasing the tension and total recovery of the initial dimensions of the sample is observed.[21−23] When the crystalline domains are already oriented along the stretching direction, that is, when the sample has already undergone the plastic deformation, the fibers show good elastic properties.

In a recent paper, an analysis of the elastic properties of sPP at different temperatures has been reported.[26] Fibers stretched at low temperatures are in the trans-planar form III, which transforms into the helical form II upon releasing the tension, whereas fibers stretched at high temperatures (60−80 °C) are in the stable helical form I and no structural transition occurs upon removing the tension.[26] The mechanical analysis of these fibers has shown that only at room temperatures the specimens show good elastic properties.[26] The elastic recovery of the samples is in part lost also at room temperature in annealed fibers, which are in the stable form I, in both the stretched and unstrained states. Upon removing the tension, a nearly total elastic recovery is observed only when the trans-planar form III transforms.[26] Only a partial elastic recovery is instead observed when no structural transition occurs. The relative amount of crystalline phase in unoriented films and in stretched and stress-relaxed fibers was found constant and not depending on the stretching temperature in the range 25−80 °C.[26]

These data strongly support the hypothesis suggested in ref 23, that the elasticity of sPP is partially linked to the enthalpy gain achieved when the tension is removed, due to the metastability, in the unstrained state, of the trans-planar form, which transforms into the stable helical form. On the other hand, an entropic factor also must play a role, due to the entangled amorphous chains which experience a reversible conformational transition between disordered (coil) and extended conformations during the stretching and relaxation process.

The origin of the non conventional elastic response of sPP to tensile stress addresses to basic questions concerning the possible mechanisms subtending elasticity in thermoplastic elastomers. In fact, while the driving force which induces the recovery of the initial dimensions in common elastomers upon releasing the stress is merely entropic,[25] in the case of sPP it is also associated with the enthalpic gain achieved when the sample is relaxed, which involves the crystal−crystal phase transition from the metastable form III to the more stable form II.[23,26]

This hypothesis is also supported by some arguments given in ref 27, concerning the formation of the isochiral form II from the trans-planar form III instead of the more stable antichiral form I, in stress relaxed sPP samples. It was argued that the crystal−crystal phase transition between form II and form III is a highly cooperative and direct process, imposed by steric constraints implying conformational and structural rearrangements of large bundles of close neighboring chains.[27]

In a recent paper,[28] we have presented preliminary results of a study of the time scale of this crystal−crystal transition, by in situ X-ray diffraction experiments with syncrotron radiation. This analysis clearly indicates that the structural transitions of sPP fibers is a fast process and occurs on the same time scale as the rate the material is stretched.[28] Moreover, the reversible phase transition between form II and form III occurs directly, without involving a third, disordered, intermediate phase. This indicates that the crystal−crystal phase transition between form II and form III is a highly cooperative process, implying collective and fast conformational and structural rearrangements of bundles

of close neighboring chains,[28] in line with the arguments given in ref 27. Such kind of phase transitions are common to alloys and steels and are said martensitic transitions.[29]

In this paper, the in situ structural analysis, during stretching−relaxation cycles, is extended to sPP samples having different stereoregularity and to unoriented films. First, the phase transitions and the associated irreversible morphological changes occurring while stretching unoriented (not previously stretched) films of sPP are followed in real time. Then, the structural evolution during stretching−relaxation cycles of sPP fiber samples is followed, within the fully elastic response regime of the material. In light of the present investigation, a possible mechanism of the solid−solid-phase transition of sPP is proposed.

Experimental Section

We have analyzed two sPP samples having different stereoregularities. The sample sPP1 was kindly supplied by ATOFINA Petrolchemical Research, while the sample sPP2 was prepared in our laboratory. They were synthesized with the classic C_s-symmetric metallocene catalyst,[1] according to standard procedure. The sample sPP1 and sPP2 are characterized by molecular weights $M_w = 1.93 \times 10^5$ ($M_w/M_n = 4.5$) and 2.13×10^5 ($M_w/M_n = 2.4$), fully syndiotactic pentad content [*rrrr*] = 78 and 93% and melting temperatures of 124 and 143 °C, respectively.

Compression-molded films (0.3 mm thick) were obtained by heating powder samples at 180 °C under a press and cooling the melt to room temperature (cooling rate 10 °C/min). The samples used for X-ray diffraction analyses were rectangular strips of a given length, 5 mm wide and 0.3 mm thick, cut from freshly prepared unoriented compression-molded films. X-ray diffraction experiments were carried out on unoriented strips (tests nos. 1 and 2), and on preoriented samples (fibers) (tests nos. 3−7). Oriented fibers were prepared by stretching unoriented compression-molded films up to a given maximum length and, then, relaxing the sample by removing the tension. The films have been cyclically stretched and relaxed several times (at least four times) before testing, until they experience fully elastic recovery in the deformation range applied in our experiments.

Wide-angle X-ray diffraction measurements were performed using monochromatic X-rays of wavelength 0.718 Å and the high flux available on the beamline ID11 at the European Syncrotron Radiation Facility (ESRF), Grenoble, France. Unoriented films and oriented fibers of a given initial gauge length were mounted on a homemade dynamometer, provided of two mobile clamps, which were moved back and forth, cyclically stretching and relaxing the material at controlled rate of 5 mm/min. The mechanical apparatus allowed automatic recording of the stress−strain curves during the experiments. The X-ray diffraction patterns were recorded in situ, while deforming the material. Each diffraction pattern was exposed 2 s on a two-dimensional CCD detector and 12 frames were recorded every minute during stretching−relaxation cycles (1 frame/5 s).

The two-dimensional (2D) data were corrected for curvature of the detector using the diffraction pattern of a specific calibration grid placed in the X-ray beam. A silicon wafer was used as external standard for calibration of the sample−detector distance. The two-dimensional X-ray patterns were processed using the FIT2D program of Dr. A. Hammersley of ESRF.

The index of crystallinity has been evaluated from X-ray fiber diffraction patterns. The 2D diffraction patterns were transformed into one-dimensional plots by performing integration along the azimuthal angle using FIT2D program (integrated profiles). The circle coordinates of the strongest reflections of unoriented film specimens of sPP were used to determine the correct beam center coordinates. The monodimensional diffraction profile of the amorphous phase was evaluated performing the same procedure with FIT2D program on a 2D X-ray diffraction pattern of atactic polypropylene. The amorphous profile was then scaled and subtracted from the X-ray diffraction profile of the crystalline samples. The index of crystallinity was then calculated from the ratio of the so-obtained crystalline diffraction area and the total area of X-ray diffraction profile.

Results and Discussion

Unoriented Films: Test Nos. 1 and 2. The X-ray diffraction patterns collected while stretching an unoriented compression-molded film of the sample sPP1 up to obtain an uniaxially oriented fiber are reported in Figure 2A (only the frames indicating the most significant changes are shown) (test no. 1). Parts B and B′ of Figure 2 plot the corresponding integrated diffraction profiles (profiles corresponding to patterns recorded every 20 s are reported). Initially, the unoriented film shows a powder pattern with typical Debye−Scherrer rings (Figure 2A, 0 strain). The corresponding integrated diffraction profile (Figure 2B, 0 strain) indicates that the sample is crystallized in the most stable form I of sPP (the peaks at $2\theta = 5.72$, 7.34, and 9.59°, correspond to $(200)_{hI}$, $(020)_{hI}$ and $(121)_{hI}$ reflections of form I (hI standing for helical form I).[5] The Bragg angles of the reflections observed in the patterns of Figure 2 are reported in Table 1. The absence of the $(211)_{hI}$ reflection at $d = 4.70$ Å ($2\theta = 8.76$°), typical of the ordered form I,[2] indicates that modifications close to the limit disordered form I are obtained.[5,14]

With increasing deformation, the diffraction intensity becomes polarized along arcs, indicating that the crystallites tend to orient with chain axes parallel to the stretching direction. At 157% deformation, the $(200)_{hI}$ and $(020)_{hI}$ reflections result mainly polarized on the equatorial layer line, whereas the $(121)_{hI}$ and $(002)_{hI}$ reflections are mainly polarized on the meridian. The deformation $\epsilon = 172\%$ is critical: in the corresponding pattern of Figure 2A, the intensities of the $(200)_{hI}$ and $(020)_{hI}$ reflections appear strongly polarized on the equator and rather broad, due to the fact that the size of the crystallites in the direction normal to the chain axis decreases during elongation. In other terms, as the strain increases, the crystallites, originally present in the material, tend to align with the chain axes parallel to the stretching direction and simultaneously are broken in the direction normal to *c*; thus, each crystallite gives rise to smaller crystallites, arranged in a mosaic-like structure with the *c* axis parallel to the stretching direction.[30]

At deformation $\epsilon = 186\%$, a X-ray diffraction pattern typical of a uniaxially oriented fiber is obtained (Figure 2A). While a not negligible amount of crystals in the helical form is still present, as indicated by the presence of the $(200)_{hI}$ reflection, a large portion of crystals in trans-planar form III is already apparent, as indicated by the arrow in Figure 2A, pointing at the strongest reflection of form III placed on the first layer line, corresponding to the periodicity $c = 5.1$ Å.[17,18] The $(020)_t$ and $(110)_t$ equatorial reflections, (t standing for trans-planar) characteristic of form III of sPP,[18] at $2\theta = 7.55$ and 8.44°, are also apparent in Figure 2A and 2B′, although hidden by the large amorphous halo centered around $2\theta = 7.4$° and by the $(020)_{hI}$ reflection at $2\theta = 7.34$°, due to the large amount of crystals in form I still present in the sample.

At 272% deformation, the last frame of Figure 2A, the sample is mainly crystallized in trans-planar form III

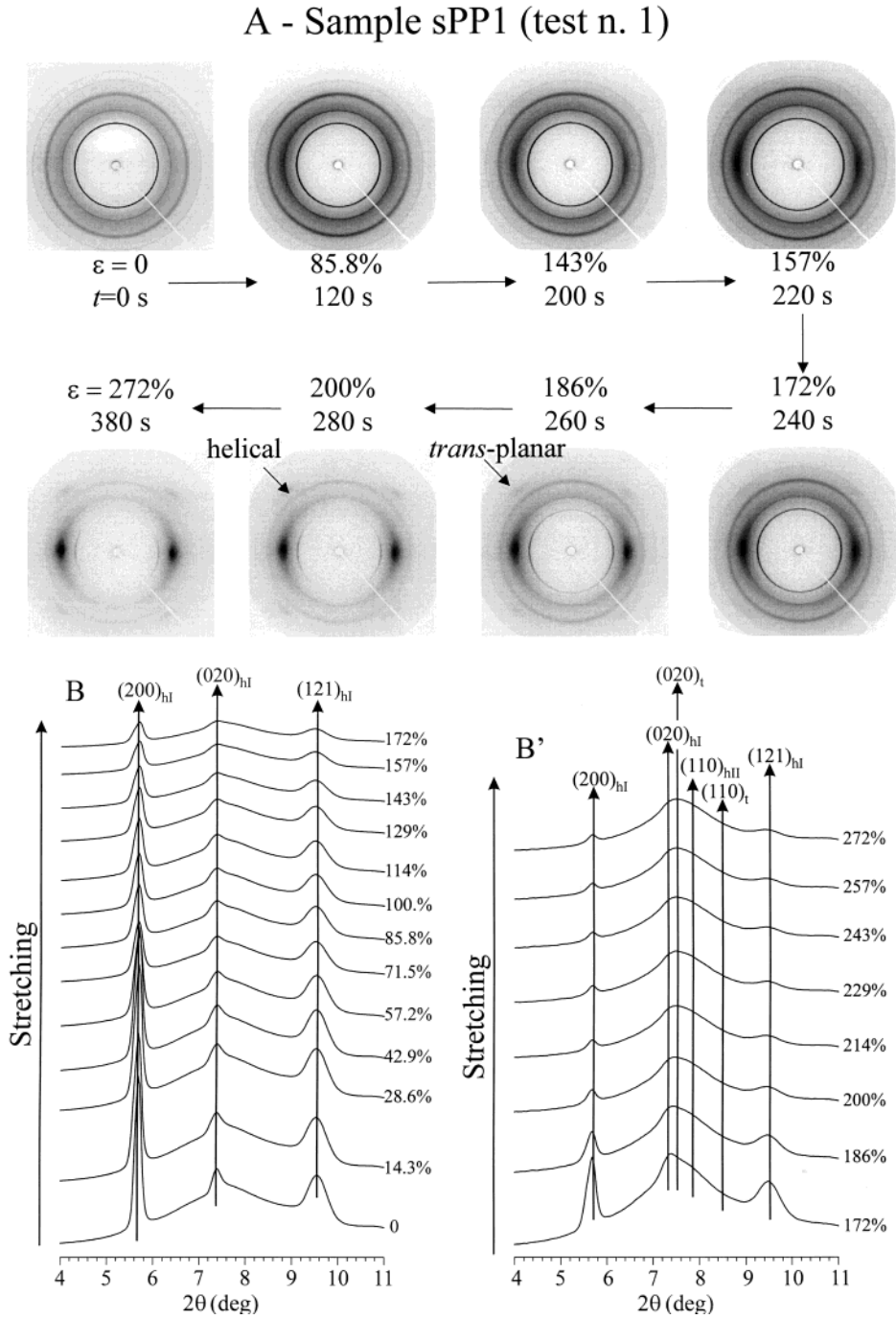

Figure 2. (A) X-ray fiber diffraction patterns of an unoriented compression-molded film of the sample sPP1, recorded in situ, while stretching the sample at rate of 5 mm/min (test no. 1, monochromatic X-ray syncrotron radiation of $\lambda = 0.718$ Å, 2 s exposure time, 12 frames/min). Only the frames outlining the most significant structural and morphological changes are reported. The deformation ϵ and the time t are indicated. The characteristic reflections of the helical form I and the trans-planar form III of sPP on the first layer line are also indicated with arrows. (B, B′) X-ray diffraction intensity profiles integrated from the two-dimensional diffraction patterns reported in A, as a function of 2θ. The label close to the profiles indicates the strain ϵ. The positions of the $(200)_{hI}$, $(020)_{hI}$, and $(121)_{hI}$ reflections of the helical form I, of the $(110)_{hII}$ reflection of form II and of the $(020)_t$ and $(110)_t$ reflections of the trans-planar form III are also indicated. The curves are reported every 20 s. The integrated profiles for $\epsilon \geq 172\%$ are reported in B′ on an enlarged intensity scale.

of sPP. It is apparent from Figure 2 that the overall diffraction intensity decreases while increasing the deformation, because the transverse section of the sample becomes progressively thinner; for this reason, the integrated diffraction profiles for strain $172 \leq \epsilon \leq 272\%$ are plotted in Figure 2B′ on an enlarged intensity scale (for comparison, the profile at 172% deformation is plotted in Figure 2, parts B and B′, in the two different scales). The index of crystallinity, initially equal to 40% for the unoriented sample, does not change during elongation. This possibly indicates that during the stretching, the crystallites in the helical form I transform directly into the trans-planar form III in correspondence to a critical strain. No evidences of temporary melting of crystals of the helical form followed by rapid recrystallization into the trans-planar form III are observed. This experiment was stopped much before the sample breaks, however at a strain inducing already a high degree of orientation of the crystals.

Table 1. Diffraction Angles (2θ) and Bragg Interplanar Distances (d) of hkl Reflections Relative to Helical Form I (Orthorhombic Unit Cell, a = 14.5 Å, b = 11.2 Å, c = 7.4 Å),[2] Form II (Orthorhombic Unit Cell, a = 14.5 Å, b = 5.6 Å, c = 7.4 Å),[5,15] and Trans-Planar Form III (Orthorhombic Unit Cell, a = 5.22 Å, b = 11.17 Å, c = 5.06 Å)[18] of sPP, Observed in the X-ray Diffraction Patterns of Figures 2, 3, 5, 6, and 8, 9, and 11[a]

form I				form II				form III			
d (Å)	$(2\theta)_{\lambda=1.5418Å}$ (deg)	$(2\theta)_{\lambda=0.718Å}$ (deg)	hkl	d (Å)	$(2\theta)_{\lambda=1.5418Å}$ (deg)	$(2\theta)_{\lambda=0.718Å}$ (deg)	hkl	d (Å)	$(2\theta)_{\lambda=1.5418Å}$ (deg)	$(2\theta)_{\lambda=0.718Å}$ (deg)	hkl
7.20	12.3	5.72	200	7.20	12.3	5.72	200	5.45	16.3	7.55	020
5.61	15.8	7.34	020	5.26	16.9	7.83	110	4.88	18.2	8.44	110
4.70	18.9	8.76	211	5.18	17.1	7.95	201	3.75	23.7	11.0	021
4.29	20.7	9.59	121	4.29	20.7	9.59	111	3.45	25.8	11.9	111
3.70	24.0	11.1	002	3.70	24.0	11.1	002				
3.59	24.8	11.5	400	3.59	24.8	11.5	400				

[a] The wavelength of the used monocromatic X-rays was 0.718 Å; for readers more familiar with conventional X-ray sources, the 2θ values of Bragg reflections corresponding to the Cu Kα radiation (λ = 1.5418 Å) are reported.

Parts A and B of Figure 3 show the X-ray diffraction patterns and the corresponding integrated intensity profiles, respectively, collected while stretching an unoriented film of the more stereoregular sample sPP2 (test no. 2). The unoriented sample is initially crystallized in the form I, as indicated by the presence of the $(200)_{hI}$, $(020)_{hI}$, $(211)_{hI}$, and $(121)_{hI}$ reflections of form I, at 2θ = 5.72, 7.34, 8.76, and 9.59° respectively, in the diffraction profile of Figure 3B (curve at $\epsilon = 0$).[2,5,13] The presence of the $(211)_{hI}$ reflection indicates that a modification close to the limit ordered model structure (Figure 1A) has been obtained. The critical strain is now located around ϵ = 90−100%; i.e., in this deformation range, the crystallites assume, abruptly, a preferred orientation with the chain axes parallel to the stretching direction; while the pattern recorded at ϵ = 91% shows still high disorientation of the crystals, the pattern recorded at 106% strain is typical of an uniaxially oriented fiber (Figure 3).

As before (test no. 1), these morphological changes are accompanied by two simultaneous phenomena: the breaking of the crystallites in direction normal to the chain axes[30] and the sudden transformation of portion of crystals previously in the helical form I into the trans-planar form III. The formation of the trans-planar form III is clearly indicated by the appearance of the typical first-layer line reflections of the trans-planar form, corresponding to a periodicity c = 5.1 Å[17,18] (indicated by the arrow in Figure 3A, pattern at ϵ = 106%) and by the presence on the equator of two maxima, centered at 2θ = 7.55 and 8.44°, corresponding to $(020)_t$ and $(110)_t$ reflections of form III[18] (Figure 3B).

Also in this case, the index of crystallinity (∼60%) of the sample does not change during the stretching. For ϵ = 136% (last frame in Figure 3A) the sample is mainly in the trans-planar form III of sPP. It is worth noting that the $(211)_{hI}$ reflection of the ordered form I, at 2θ = 8.76° (Figure 3B), first disappears, while stretching the sample. We recall that the intensity of this reflection is strongly affected by the presence of structural disorder in the alternation of helices of opposite chirality along the a and b axis of the unit cell, typical of the limit ordered model structure of form I (Figure 1A).[2,14] With increasing the strain, indeed, the crystalline lamellae break into fragments which become progressively smaller; this, in turn, destroys the long range order in the alternation of enantiomorphous helices, inducing progressive decrease of the intensity of $(211)_{hI}$ reflection in the patterns of Figure 3.

The stress−strain curves recorded while stretching the unoriented films of sPP1 and sPP2 samples in tests nos. 1 and 2, are compared in Figure 4, curves a and b, respectively (the experiment for the sample sPP2 was interrupted for ϵ = 160%; the dashed portion of curve b plots the extrapolated values). The whole stress−strain curves up to the break for unoriented films of sPP samples having analogous characteristics as those of the samples utilized in the present analysis are reported in Figure 5 of ref 23. The curves a and b of Figure 4 correspond to typical stress−strain curves of thermoplastic polymers. At small strain, the stress (σ) increases linearly with strain and the material deforms elastically, and then σ reaches a maximum value, corresponding to the yielding point of the material; for higher deformation, σ remains constant (up to the break), and the sample deforms plastically.[24] Upon release of the tension, both samples recover only partially the initial dimensions, in agreement with previous observations that manufactures of highly stereoregular sPP samples are poorly elastic when stretched from the unoriented state.[23] Figure 4 shows that the stress−strain curve of the sample sPP2 is entirely shifted toward higher σ values with respect to the curve of the sample sPP1, because of the higher degree of crystallinity of the sample sPP2.

During stretching, when the critical value of the strain is achieved, both samples undergo abrupt structural and morphological transformations. The critical strain corresponds to ∼200% for the sample sPP1 and ∼100% for sPP2. Therefore, for the most stereoregular sample sPP2 (test no. 2), the transformation of the helical form I into the trans-planar form III (accompanied by a sharp increase of degree of orientation in the sample) starts at values of strains much below the critical strain observed for the analogous transformations occurring for the less stereoregular sample sPP1 (test no. 1). From Figure 4, it is apparent that this corresponds to apply values of tensile stress of ∼8 and ∼12 MPa for the samples sPP1 and sPP2, respectively. For tensile stress in the range 8−12 MPa the crystalline domains in helical form become unstable and transform into the trans-planar form III. Since the stress value corresponds to the plateau zone of the stress−strain curve of unoriented films (see Figure 4), the exact value of the critical stress depends on the rigidity of the sample. The rigidity, in turn, depends on the degree of steoreoregularity, which influences the amount of crystallinity achieved in similar crystallization conditions. The more stereoregular sample sPP2 is, indeed, more crystalline and more rigid than the less stereoregular sample sPP1.

Oriented Fibers: Tests Nos. 3—7. Figures 5−7 illustrate the typical results obtained in one of the several experiments performed on fibers of the sample

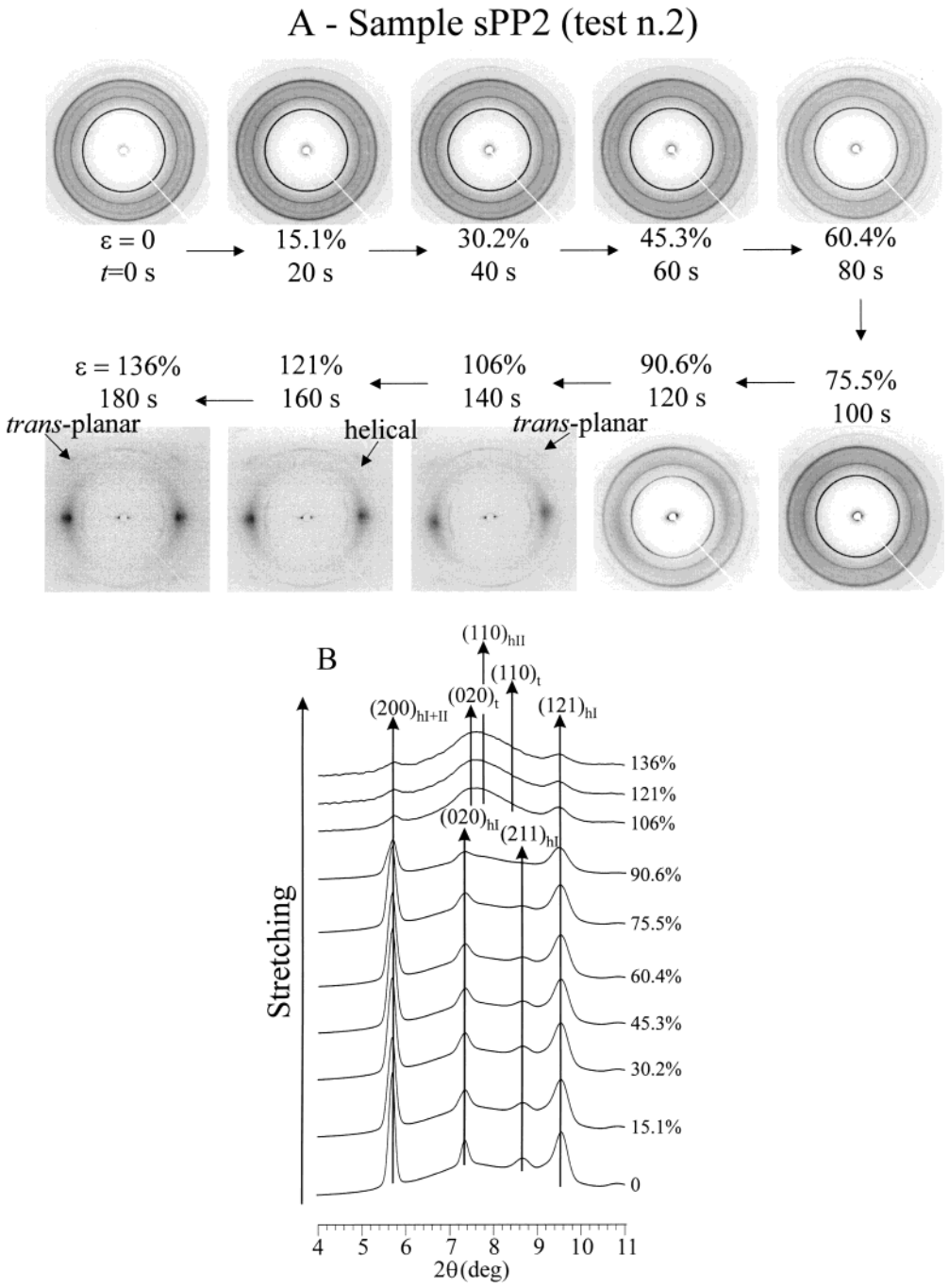

Figure 3. (A) X-ray fiber diffraction patterns of an unoriented compression-molded film of the sample sPP2, recorded in situ, while stretching the sample at rate of 5 mm/min (test no. 2, monochromatic X-ray syncrotron radiation of $\lambda = 0.718$ Å, 2 s exposure time, 12 frames/min). Only the frames outlining the most significant structural and morphological changes are reported. The deformation ϵ and the time t are indicated. The characteristic reflections of helical form I and trans-planar form III of sPP on the first layer line are also indicated with arrows. (B) X-ray diffraction intensity profiles integrated from the two-dimensional diffraction patterns reported in A, as a function of 2θ. The label close to the profiles indicates the strain ϵ. The positions of $(200)_{hI}$, $(020)_{hI}$, and $(121)_{hI}$ reflections of the helical form I, of the $(110)_{hII}$ reflection of form II, and of the $(020)_t$ and $(110)_t$ reflections of the trans-planar form III are also indicated. The curves are reported every 20 s.

sPP1, cyclically stretched and immediately relaxed at controlled rate, within a deformation range corresponding to a fully elastic response of the material (test no. 3). As reported in the experimental part, oriented fibers have been prepared by stretching compression-molded films up to a given strain (as in tests nos. 1 and 2) and then removing the tension. Before recording the test no. 3 (Figures 5−7), the fibers have been cyclically stretched and relaxed at least four times. The X-ray fiber diffraction patterns and the corresponding diffraction profiles read along the equatorial line (after subtraction of the amorphous contribution) are reported in Figures 5 and 6, respectively.

The patterns of Figures 5 and 6 were recorded while stretching the fiber from 0 to 52.6% strain (Figures 5A and 6A) and relaxing the tension at controlled rate from 52.6% to 0 strain (Figures 5B and 6B). The stress−strain curves recorded while performing the experiment, are reported in Figure 7. They correspond to typical stress−strain hysteresis curves already reported in the literature for sPP samples having analogous stereoregularity.[21−23] The Bragg angles 2θ and the Bragg

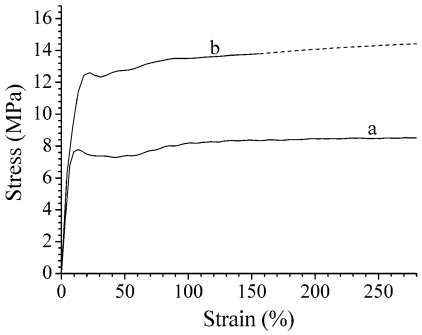

Figure 4. Stress−strain curves recorded while stretching unoriented films of samples sPP1 (curve a) and sPP2 (curve b) in tests nos. 1 and 2, respectively. Both experiments were stopped long before breaking of the samples.

distances of the *hkl* reflections present in the X-ray patterns of Figures 5 and 6 are reported in Table 1. We have checked that the index of crystallinity of the sample over consecutive cyclic stress-relaxation runs remains constant at nearly 40%, as in the original unoriented film (test no. 1).

In the unstrained state, the fiber is basically in the isochiral helical form II, as shown by the presence of strong $(111)_{hII}$ reflection at $d = 4.29$ Å, (labeled "helical" in Figure 5A, $\epsilon = 0$), and by strong equatorial maxima at $d = 7.20$ and 5.26 Å ($2\theta = 5.72$ and 7.83°, respectively, Figure 6A, curve for $\epsilon = 0\%$), which correspond to the reflections $(200)_{hII}$ and $(110)_{hII}$, respectively, of form II of sPP[15,16] (the symbol hII standing for helical form II). This indicates, in agreement with the results reported in the literature,[23] that stretching unoriented samples of sPP in the stable helical form I, an irreversible crystal−crystal phase transition from form I into form III occurs (tests nos. 1 and 2, Figures 2 and 3). The trans-planar form III transforms into the isochiral form II of sPP, in the strained fibers upon removing the tension. We recall that sPP is poorly elastic, when stretched from unoriented state.[23]

The unstrained fiber ($\epsilon = 0$) also includes a not negligible fraction of crystals in the trans-planar conformation. This is indicated by the presence in the pattern of Figure 5A ($\epsilon = 0$) of off-equatorial reflections corresponding to chain periodicity $c = 5.1$ Å (the strongest first layer line reflection arising from these crystals is labeled "trans-planar" in Figure 5A)[17,18] and by the strong asymmetric peak on the equator, centered on the $(110)_{hII}$ reflection at $2\theta = 7.83°$, spanning the 2θ region between 7.5 and 8.5° (Figure 6A, curve for $\epsilon = 0$), due to the contribution of the $(020)_t$ and $(110)_t$ reflections of the trans-planar form III.

As shown in Figures 5A and 6A, for strain lower than a characteristic value, $\epsilon_c \approx 20\%$ (corresponding to $\sigma_c \approx 10$ MPa, Figure 7), we do not observe any significant change in the X-ray diffraction patterns. For higher deformations, $\epsilon > \epsilon_c$ ($\sigma > \sigma_c$), the intensity of $(200)_{hII}$ reflection gradually decreases with increasing ϵ, while the intensities of $(020)_t$ and $(110)_t$ reflections ($2\theta = 7.55$ and 8.44°, respectively, Figure 6A), typical of form III,[18] increase. This indicates that with increasing deformation, the relative amount of crystals in form II decreases and the content of crystals of form III increases. Since the index of crystallinity does not change, this indicates that a stress-induced phase transition from form II into form III occurs when the sample is stretched above a characteristic deformation value. At 52.6% deformation, ∼70% of the material originally in the helical conformation, transforms into form III (Figures 5A and 6A). The degree of orientation of helical crystals does not greatly increase while stretching the material (Figure 5A), and a high degree of orientation of crystals, with trans-planar chains parallel to stretching direction, is achieved in the fully strained state (see the pattern at $\epsilon = 52.6\%$ in Figure 5A).

The structural and morphological changes occurring during the stretching, are reversible. The crystals in the trans-planar form III gradually transform back into the helical form as the tensile stress is released (Figures

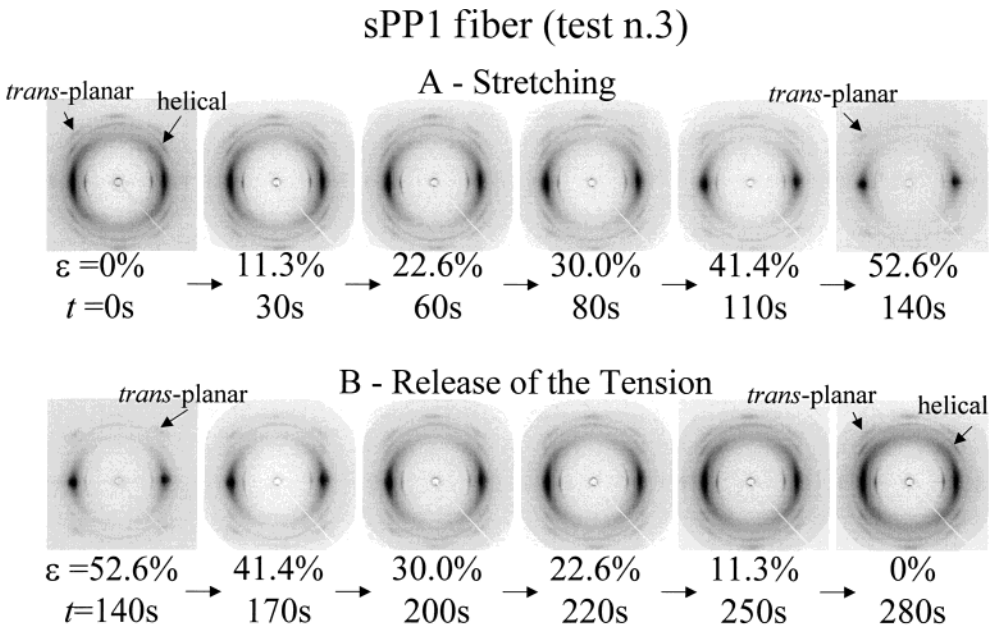

Figure 5. X-ray fiber diffraction patterns of a uniaxially drawn fiber of the sample sPP1, recorded in situ during cyclic elongation and recovery (deformation rate, 5 mm/min), within the elastic deformation range (test no. 3, monochromatic X-ray syncrotron radiation of $\lambda = 0.718$ Å, 2 s exposure time, 12 frames/min). Only the frames outlining the most significant structural changes are reported. (A) The patterns were recorded while stretching the sample; (B) the patterns were recorded while releasing the tension. The deformation ϵ and the time t are indicated. The characteristic reflections of helical form II and trans-planar form III of sPP on the first layer line are also indicated with arrows.

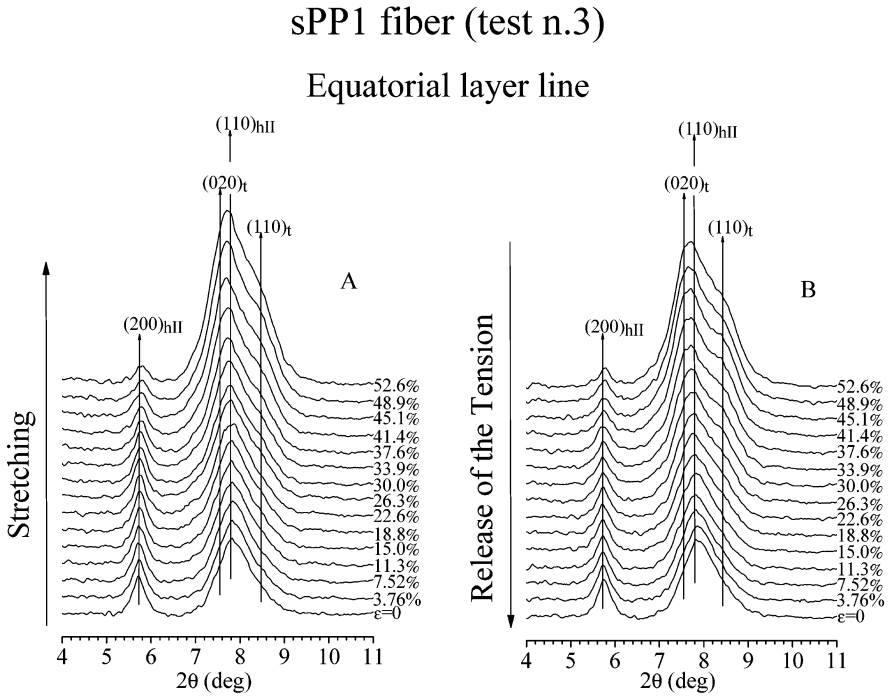

Figure 6. (A, B) X-ray diffraction intensity profiles read along the equatorial layer line of the two-dimensional fiber diffraction patterns of Figure 5, parts A and B, respectively, as a function of 2θ diffraction angle, after subtraction of the amorphous contribution (test no. 3). The label close to the profiles indicates the strain ϵ. The position of the $(200)_{hII}$ and $(110)_{hII}$ reflections of helical form II and of the $(020)_t$ and $(110)_t$ reflections of the trans-planar form III are also indicated. The curves are reported every 10 s.

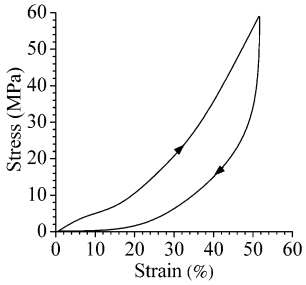

Figure 7. Stress−strain curves recorded while cyclically stretching the fiber of test no. 3 (sample sPP1) and releasing the tension at a controlled rate of 5 mm/min according to directions indicated by the arrows.

5B and 6B). The $(020)_t$ and $(110)_t$ reflections of the trans-planar form III, indeed, gradually disappear and the intensities of the $(200)_{hII}$ and $(110)_{hII}$ reflections diagnostic of helical form II increase, while releasing the tension (Figure 6B). Below a critical strain (i.e., for $\epsilon_c < 20\%$, Figure 6B), the sample is almost fully helical. At the end of test no. 3, the oriented fiber of the sample sPP1 completely recovers the initial dimensions (Figure 7) and results in a mixture of crystals of form II and form III (Figure 5B, $\epsilon = 0$), in the same relative amount as at the beginning of the experiment (Figure 5A, $\epsilon = 0$).

Figures 8−10 show the results obtained in a typical experiment performed on a fiber of the more stereoregular sample sPP2, cyclically stretched (from $\epsilon = 0$ to 41.1%) and then immediately relaxed at a controlled rate (from $\epsilon = 41.1\%$ to 0, test no. 4). The sample is fully elastic in this deformation range. The X-ray fiber diffraction pattern and the corresponding diffraction profiles read along the equator (after subtraction of the amorphous contribution) are reported in Figures 8 and 9, respectively. The stress−strain hysteresis curves recorded while performing the diffraction experiment are reported in Figure 10. The overall index of crystallinity does not change during the mechanical cycle in the test no. 4 and amounts to ≈60%, as in the original unoriented film of sample sPP2 (test no. 2, Figure 3). Furthermore, the reflections corresponding to the crystalline forms involved during the mechanical cycle in test no. 4 are more sharp and narrow than those shown in test no. 3 by the oriented fiber of the sample sPP1, indicating that the crystals in the sample sPP2 are now bigger and more ordered.

As in the case of the sample sPP1 (test no. 3, Figures 5 and 6) in the unstrained state, the fiber of sample sPP2 is mostly in the helical form II, as indicated by the presence of $(111)_{hII}$, $(200)_{hII}$, and $(110)_{hII}$ reflections typical of the isochiral helical form II[15,16] (Figure 8A and 9A, $\epsilon = 0$). A small amount of crystals of trans-planar form III is also present as indicated by the presence of reflections on the first-layer line corresponding to chain periodicity $c = 5.1$ Å[17,18] and by the presence of the shoulders of the $(110)_{hII}$ reflection ($2\theta = 7.83°$) at $2\theta = 7.55$ and 8.44°, corresponding to the $(020)_t$ and $(110)_t$ reflections, respectively, of form III[18] (Figures 8A and 9A, $\epsilon = 0$; see also Table 1). The critical value of the strain at which the transition of form II into form III starts ($\epsilon_c \approx 10\%$), is now shifted toward values of ϵ lower than that observed for the sample sPP1 (Figure 6A). The corresponding value of the critical strain is 12 MPa (Figure 10). As in the case of the sample sPP1 in test no. 3, a stress-induced phase transition from form II into form III occurs when the sample is stretched above this critical value of deformation. It is apparent, indeed, from Figures 8A and 9A, that for $\epsilon > 10\%$ ($\sigma > 12$ MPa), the intensity of $(200)_{hII}$ reflection of the helical form gradually decreases with increasing ϵ, while the intensities of $(020)_t$ and $(110)_t$ reflections ($2\theta = 7.55$ and 8.44°, respectively, Figure 8A), typical of form III,[18] increases. Also in this case the index of crystallinity remain constant over the stretching−relaxation runs.

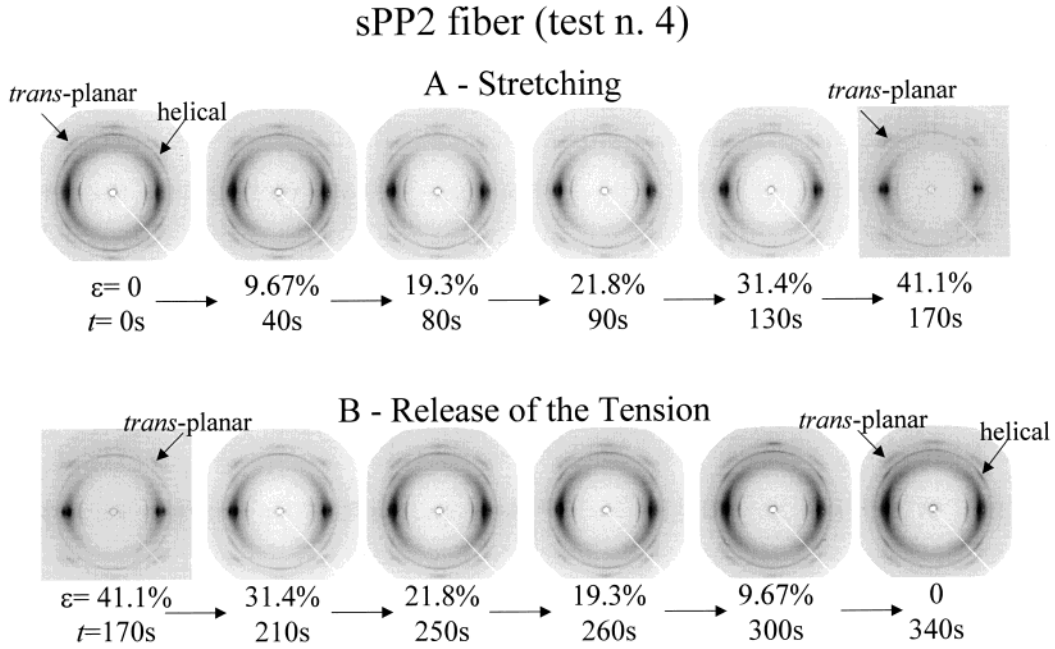

Figure 8. X-ray fiber diffraction patterns of an uniaxially drawn fiber of sample sPP2, recorded in situ during cyclic elongation and recovery (deformation rate, 5 mm/min), within the elastic deformation range (test no. 4, monochromatic X-ray syncrotron radiation of $\lambda = 0.718$ Å, 2 s exposure time, 12 frames/min). Only the frames outlining the most significant structural changes are reported. (A) The patterns were recorded while stretching the sample; (B) the patterns were recorded while releasing the tension. The deformation ϵ and the time t are indicated. The characteristic reflections of helical form II and trans-planar form III of sPP on the first layer line are also indicated with arrows.

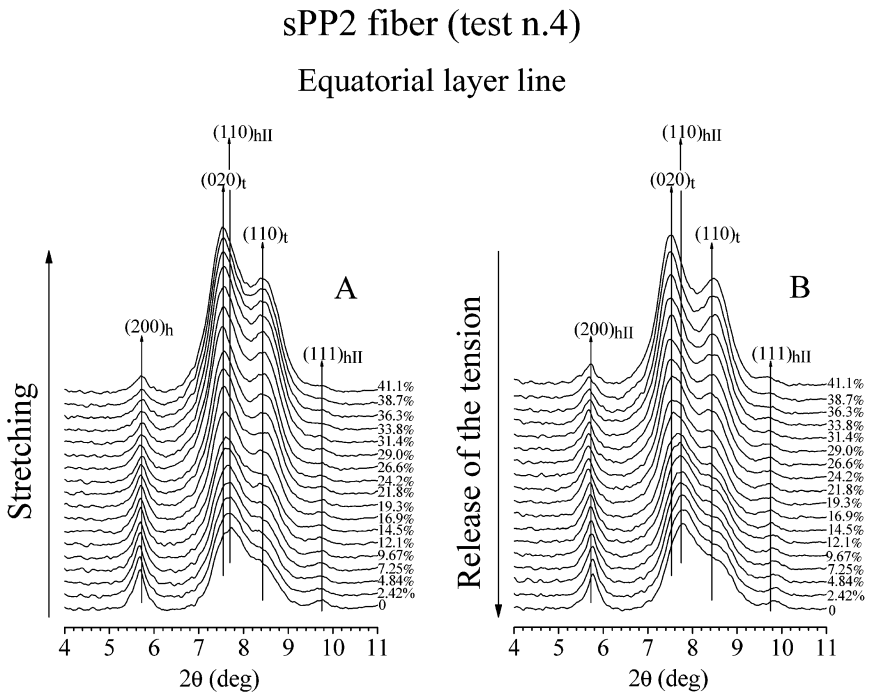

Figure 9. (A, B) X-ray diffraction intensity profiles along the equatorial layer line of the two-dimensional fiber diffraction patterns of Figure 8A and 8B, respectively, as a function of 2θ diffraction angle, after subtraction of the amorphous contribution (test no. 4). The label close to the profiles indicates the strain ϵ. The positions of the $(200)_{hII}$, $(110)_{hII}$, and $(111)_{hII}$ reflections of helical form II and of the $(020)_t$ and $(110)_t$ reflections of the trans-planar form III are also indicated. The curves are reported every 10 s.

At 41.1% deformation, nearly 70% of the material originally in the helical form transforms into form III (Figures 8A and 9A). Also in this case, the degree of orientation of helical crystals does not greatly increase while stretching the material (Figure 8A), whereas a high degree of orientation of crystals with trans-planar chains parallel to stretching direction, is achieved in the fully strained state (see the pattern for $\epsilon = 41.1\%$ in Figure 8A).

During the relaxation run at controlled rate, the crystals in trans-planar form III, gradually transform back into the helical form II as the tensile stress is released (Figures 8B and 9B). Indeed, the intensities of the $(020)_t$ and $(110)_t$ reflections of the trans-planar form III gradually decrease and the intensities of the $(200)_{hII}$ and $(110)_{hII}$ reflections of the helical form II increase, while releasing the tension. In addition, the sample becomes progressively less oriented. Below a

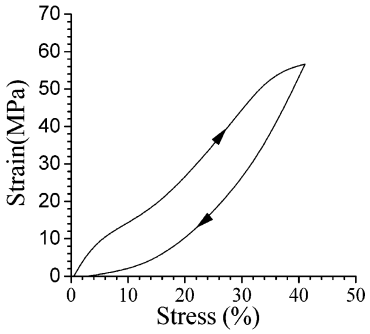

Figure 10. Stress−strain curves recorded while cyclically stretching the fiber of test no. 4 (sample sPP2) and releasing the tension at a controlled rate of 5 mm/min, according to directions indicated by the arrows.

critical strain (i.e., for $\epsilon_c < 10\%$ and $\sigma \approx 10$ MPa, Figure 10), the fraction of crystals transformed from the helical form into trans-planar form during the stretching transforms back into form II during the relaxation. At the end of test no. 4 (Figure 8B, $\epsilon = 0$), the sample completely recovers the initial dimensions and results in a mixture of crystals of form II and form III, in the same amount as at the beginning of the test (Figure 8A, $\epsilon = 0$).

In both tests no. 3 and no. 4, the X-ray diffraction patterns of samples stretched up to a given strain ϵ (Figure 5A and 8A) are practically coincident with the patterns at the same value of the strain ϵ during the relaxation (Figures 5B and 8B). Furthermore, we have checked that the X-ray diffraction patterns of Figures 5 and 6, for the sample sPP1, and Figures 8 and 9, for the sample sPP2, and the stress−strain curves of Figures 7 and 10 are coincident to those recorded during analogous elongation-relaxing cyclic tests, over more than 12 consecutive runs.

In conclusions, as already observed in ref 23, the crystal−crystal phase transition between the isochiral helical form II and the trans-panar form III of sPP is reversible, and a total recovery of the initial dimensions of the sample is observed when the tension is removed. Thus, oriented samples of sPP show good elastic behavior.

Moreover, in agreement with the results reported in ref 28 for oriented sPP samples, the transition of form II into form III occurs during the stretching in correspondence to characteristic values of stress−strain parameters. At values of strain below the characteristic values of the strain, the samples are almost fully in the helical form. The characteristic values of the strain are $\epsilon_c \approx 20\%$ for the sample sPP1 and $\epsilon_c \approx 10\%$ for sPP2. Therefore, for the more stereoregular sample sPP2 (test no. 4), the transformation of form I into form III (accompanied by an increase of the degree of orientation) starts for a strain much below the critical strain observed for the analogous transformations occurring for the less stereoregular sample sPP1 (test no. 3). The values of the critical stress corresponding to these values of the critical strain are ≈10 MPa for sPP1 and ≈12 MPa for sPP2, during stretching (Figures 7 and 10). Lower values of the critical strain are instead observed during relaxation, because of the non null hysteresis (Figures 7 and 10). As for unoriented samples, the critical stress inducing the structural transition of the helical form into the trans-planar form in sPP is in the range 8−12 MPa, and the exact value depends on the degree of steoreogularity of the sample, which in turn influences the degree of crystallinity and the relative amount of structural disorder in the crystals. In other words, the major determining parameter for the structural transition between form II and form III is the applied tensile stress, rather than the strain value. These observations are in agreement with results reported in recent papers by Choi and White.[31−33] In ref 31, in particular, Choi and White have studied the structure development in melt spinning process of sPP. It was found that the transition of the helical form I into the trans-planar form III starts at a spinline stress level of about 6−9 MPa, regardless of molecular weight, melt temperature, and cooling rate; moreover, the spinline stress level was found to be the major determining parameter for obtainment of high degree of orientation in the resulting sPP fibers. The critical stress found in ref 31 is slightly lower than the value found in the present investigation, probably because the sPP samples analyzed in ref 31 were less stereoregular than our samples.

The results of our in situ analysis provide clear evidences that the structural evolution of sPP is a fast process and occurs on the same time scale as the rate the material is stretched.

As a further check, the sample of test no. 4, once relaxed, was stretched again up to $\epsilon = 29\%$ and then the tension was abruptly removed (test no. 5). The X-ray fiber diffraction patterns were recorded every 5 s during this experiment. The X-ray diffraction patterns and the corresponding diffraction profile read along the equator, are reported in Figure 11A and B, respectively (only the frames indicating the most significant changes are shown in Figure 11A). As in test no. 4, the structural transition of form II into form III starts at $\epsilon \approx 10\%$. Starting from this moment, the crystals of form II gradually transform into form III while stretching. After 120 s from the beginning of the experiment, at $\epsilon = 29\%$ (pattern d in Figure 11A), the tension is abruptly removed. It is apparent from Figure 11 that crystals of form III, formed during the stretching, transform back into form II instantaneously (pattern e of Figure 11A and profile at 125 s, $\epsilon = 0$, in Figure 11B). An instantaneous recovery of the initial dimensions of the sample is also observed. It is worth noting that the diffraction patterns at $\epsilon = 0$ at the end (125 s) and at the beginning of the experiment (0 s) in Figure 11, parts A and B, are practically coincident.

This result clearly indicates that the reversible phase transition between form II and form III occurs instantaneously and directly, without involving a third disordered, intermediate phase; i.e., as suggested in ref 27, it is a cooperative process, involving conformational and structural rearrangements of bundles of close neighboring chains in short time. Moreover, these data suggest that the crystal−crystal phase transition between form II and form III in sPP is a martensitic transition, with associated characteristic values of stress−strain parameters. As in the case of martensitic transitions occurring in alloys and steels, also for sPP, the critical value of the stress−strain parameters depend on the temperature; for instance, as shown in ref 26, for temperatures higher than 60 °C the helical form does not transform into form III upon stretching.

Recent energetic analyses have shown that form II of sPP is more stable than form III by ≈0.51 kcal/mol monomeric units.[34] Therefore, while the driving force leading the conventional elastomers to recover the

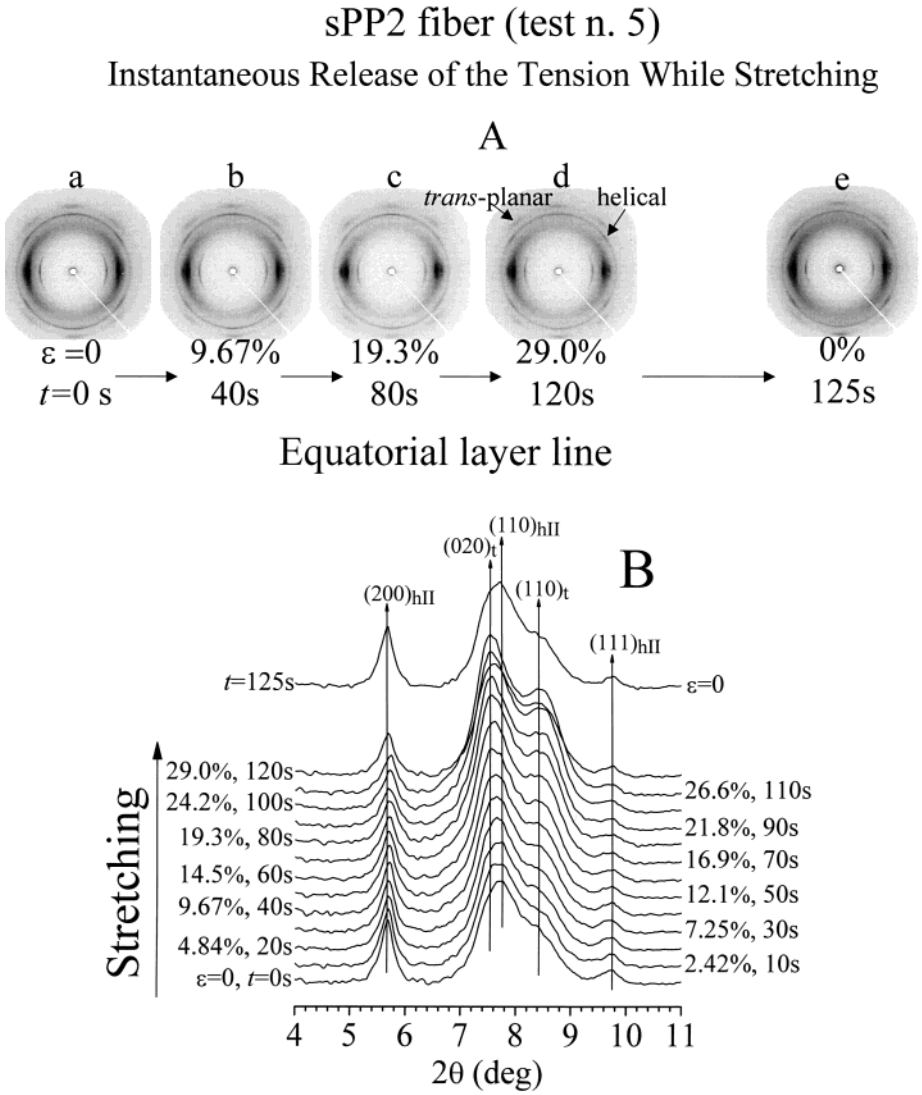

Figure 11. (A) X-ray fiber diffraction patterns of an uniaxially drawn fiber of the sample sPP2, recorded in situ during stretching (deformation rate, 5 mm/min, patterns a−d). At $\epsilon = 29\%$ (pattern d), the tension is abruptly removed and the diffraction pattern (pattern e) immediately recorded (test no. 5, monochromatic X-ray syncrotron radiation of $\lambda = 0.718$ Å, 2 s exposure time, 12 frames/min). Only the frames outlining the most significant structural changes are reported. The deformation ϵ and the time t are indicated. The characteristic reflections of helical form II and trans-planar form III of sPP on the first layer line are also indicated with arrows. (B) X-ray diffraction intensity profiles along the equatorial layer line of the two-dimensional fiber diffraction patterns of Figure 11A, as a function of 2θ diffraction angle, after subtraction of the amorphous contribution (test no. 5). The labels close to the profiles indicate the strain ϵ and the time t. The positions of the $(200)_{hII}$, $(110)_{hII}$ and $(111)_{hII}$ reflections of helical form II and of the $(020)_t$ and $(110)_t$ reflections of the trans-planar form III are also indicated.

initial dimensions is merely entropic, in the case of sPP, elasticity is also assisted by the enthalpic gain achieved when the sample is relaxed. When the tension is removed, both the enthalpic factor, due to the structural transition in the crystalline region, and the entropic factor, due to the conformational transition of the entangled chains in the amorphous phase, contribute to the elastic recovery of the sPP fibers.

In our opinion the rather small crystalline aggregates actively participate in the elasticity of sPP, locally acting as microscopic engines.[28] The chains in the amorphous regions are possibly well oriented and are in an extended conformation in the stretched state and experience a reversible conformational transition between the disordered (coil) and extended conformations when the samples are repeatedly stretched and relaxed. These chains are also highly entangled and connect different crystals, as tie chains.[30] In the crystalline domains the structural transition occurs during the mechanical cycles. During deformation, the chains in the amorphous regions assume extended conformations and tend to orient parallel to the stretching direction, and the crystalline aggregates tend to assume a preferred orientation with the chain axes parallel to the stretching direction. When the crystalline aggregates experience a tensile stress higher than a critical value, a crystal−crystal phase transition from the helical form II into the trans-planar form III occurs and the size of the crystal increases by 38% along the chain axis direction[23,28] (the periodicity per monomeric unit increases from 7.4/4 Å for the helical form, to 5.1/2 Å for the trans-planar form, with 7.4 and 5.1 Å the chain axes of the helical form II and the trans-planar form III, respectively, corresponding to a relative increase of 38% = 100-(5.1/2 − 7.4/4)/(7.4/4)).

During the relaxation step, when a given crystal experiences a stress below a critical value, form III becomes unstable and transforms instantaneously into

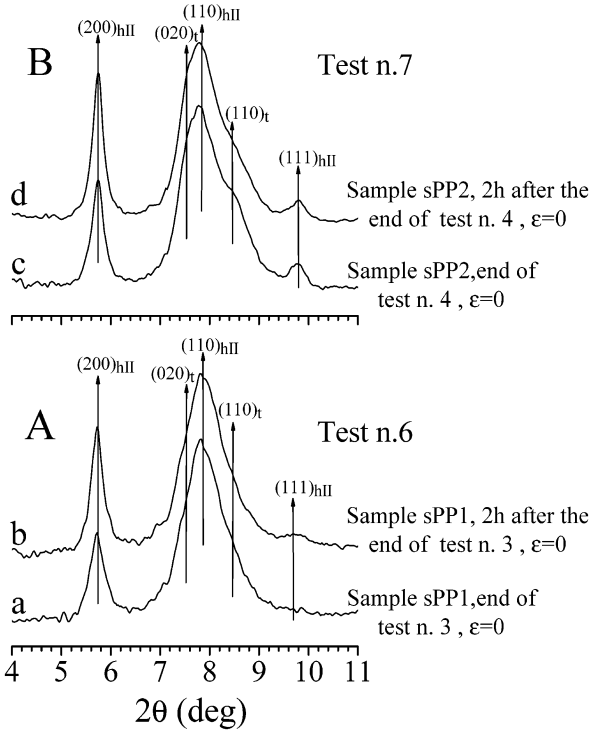

Figure 12. Comparison between X-ray equatorial diffraction profiles of the stress-relaxed fibers of samples sPP1 (A) and sPP2 (B) at the end of tests nos. 3 and 4, respectively (profiles a and c), and 2 h after the end of the experiments (profiles b and d).

the more stable form II, and each crystal, locally, shrinks by 38% along the chain axis direction.[23,28] Since the enthalpy change in this transition is negative, the heat of transition, in turn, induces an abrupt conformational transition of the amorphous material placed in the surrounds; the amorphous springs assume suddenly less extended conformations generating a sort of chain reaction, which rapidly involve the whole material. According to this idea, elasticity in sPP would not be merely entropic as in conventional elastomers but also enthalpic.

The dimension of crystallites and the amount of structural order which develops in the crystalline modifications involved during stretching−relaxation cyclic tests is higher for the more stereoregular sample sPP2 than for the less stereoreguar sample sPP1. In both cases the elastic response of the sample during cyclic deformation and relaxing experiments is instantaneous, and the reversible crystal−crystal phase transition between form II and form III occurs on the same time scale as the rate the sample is deformed. Nevertheless, in tests nos. 3−5 oriented fibers of sPP still show a not negligible amount of crystals in the transplanar form III, once the tension is removed (Figure 5, 6, 8, 9, and 11). This crystalline modification is unstable in absence of a tensile stress, and keeps transforming into the helical form II, in longer time. This is shown in Figure 12, which compares the equatorial diffraction profiles of the unstrained fiber samples sPP1 (Figure 12A) and sPP2 (Figure 12B) at the end of tests nos. 3 and 4, respectively (curves a and c, Figure 12), with those of the same fiber samples kept for 2 h at room temperature in the unstrained state (curves b and d, Figure 12). A neat increase of the intensity of the $(200)_{hII}$ reflection is observed, whereas the two shoulders of the $(110)_{hII}$ peak at $2\theta = 7.83°$, corresponding to the $(020)_t$ and $(110)_t$ reflections of trans-planar form III of sPP, become less pronounced (compare profiles a and c with profiles b and d, respectively). The delayed transition of crystals in form III into form II in the stress-relaxed fibers also implies further shrinkage of the sample length. Most likely, the crystals of form III which do not transform back into form II instantaneously while releasing the tension are located in strained zones of the material; when the material is left to relax at room temperature, these crystals also transform into form II.

A Possible Mechanism of the Martensitic Phase Transition between Form II and Form III of sPP. It is worth noting that form II is not the most stable form of sPP;[5,15] it is based on packing of isochiral 2-fold helical chains into an orthorhombic unit cell (Figure 1B).[15] The most stable crystalline form of sPP is form I,[2] characterized by a packing of antichiral helices along both *a* and *b* axes (Figure 1A).[2,5,13] Form I is the common form of sPP obtained in powder samples by crystallization from the melt[5,14] and in single crystals from solution.[2−4] At high crystallization temperatures ordered modifications close to the limit ordered model structure of Figure 1A are obtained.[2,14] At low crystallization temperatures disordered modifications characterized by the presence of disorder in the alternation of right- and left-handed helices along the *a* and *b* axes are obtained.[14] These disordered modifications also include disorder in the stacking of *bc* layers of chains along *a*, characterized by shift of the layers of *b*/4 along *b* (*b*/4 shift disorder) generating local situations of packing of close neighboring chains as in form II of sPP.[3,4,14] Form II may be obtained in powder samples upon quench precipitation from solution (disordered modifications including kink−band disorder),[35,36] crystallization from the melt at high pressures,[37] and in fiber samples initially in form III upon removing the tension.[16,23] When the crystallization of form III in oriented fibers is prevented, as for instance by stretching at high temperature[26]or in copolymers of sPP with butene comonomeric units,[38] form II does not form anymore. The question why the isochiral form II occurs instead of the more stable antichiral counterpart (form I) in stress-relaxed sPP fibers initially in form III, is intriguing. In ref 27 we suggested the hypothesis that the evolution of form III fibers into form II is imposed by conformational and steric constraints, and the isochirality of the resulting helical phase was taken as an indication that the transformation is a cooperative process.

As shown in the previous session, the crystal−crystal phase transition between form III and form II of sPP is a fast and direct process, not involving any intermediate disordered phase during the transformation. This suggests that this phase transition is a cooperative process, occurring through instantaneous and simultaneous conformational and structural rearrangements of close neighboring chains, involving the whole ordered domains, in agreement with the hypothesis suggested in ref 27.

As argued in ref 27, the generation of a helix structure requires the introduction of G^+ or G^- bonds in an all-trans chain during the crystal−crystal phase transition from form III to form II. This implies a modification in chain direction and, ultimately, generation of a helix with a larger cross section than that of the initial conformation. Such process also involves very major

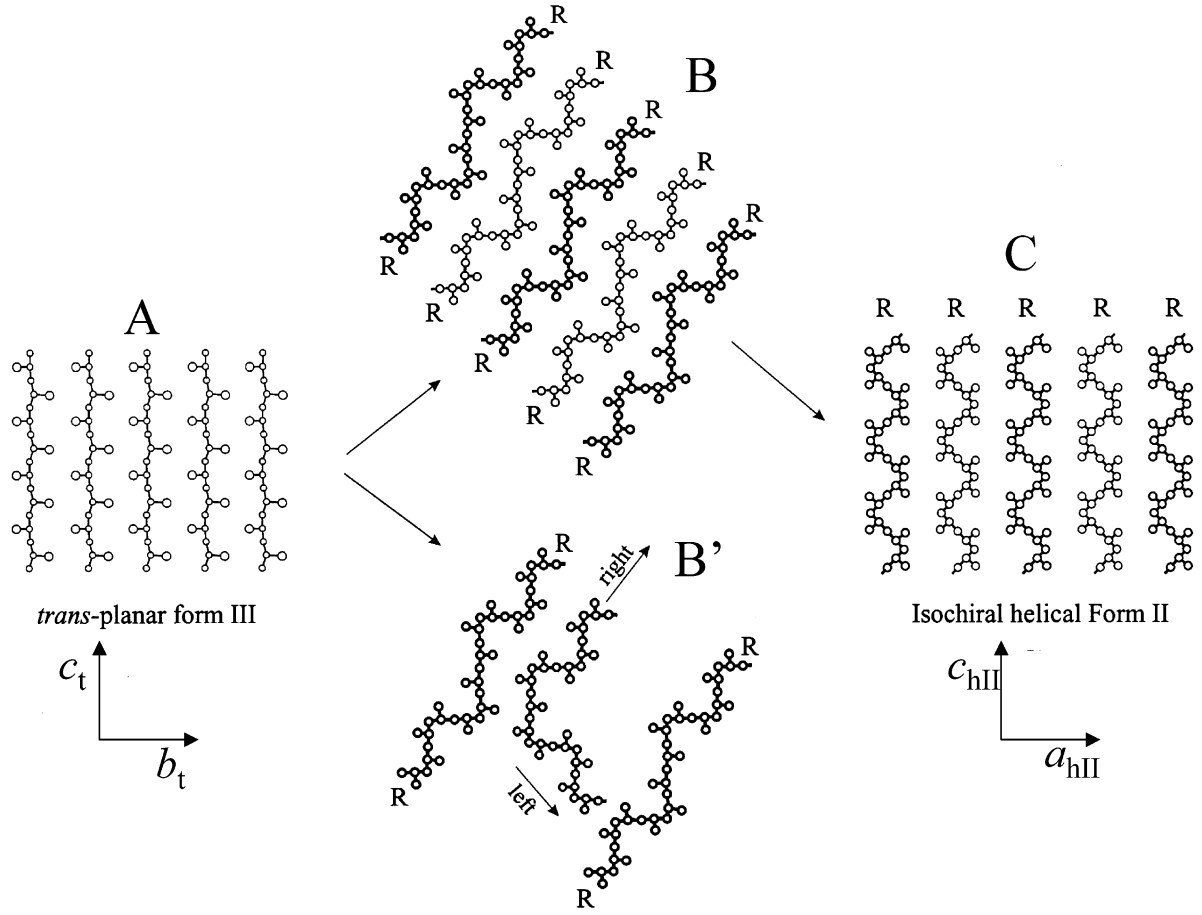

Figure 13. Possible mechanism for the martensitic phase transition between form III and form II of sPP. (A) sPP chains in trans-planar conformation, arranged as in the form III, in a projection parallel to the chain axes. (B) Right-handed helical portions of chains formed in unison along sPP chains, connected by portions of chains in trans-planar conformation, clustered in planes as in the model of kink−band disorder of form II of sPP,[35,36] illustrating a transient state of the crystalline aggregate of chains originally in form III transforming into form II. (B′) The formation of helical portions of chains having opposite chirality within the same ordered domain is forbidden because the two stems would be oriented at right angle each other, producing steric interactions with neighboring chains. (C) sPP chains in $(TTGG)_n$ helical conformation, arranged as in the isochiral form II, in a projection parallel to the chain axes.

molecular readjustments which, to take place, must be direct and cooperative.

A possible mechanism for the crystal−crystal phase transition from form III into form II of sPP, implicitly suggested in ref 27 and supported by the results of the present investigation, is illustrated in Figure 13. The relative arrangement of sPP trans-planar chains in a crystalline aggregate of form III is shown in Figure 13A. Upon release of the tension, form III is unstable and transforms into the more stable isochiral form II (Figure 13C). This transition implies the generation of ...TTG^+G^+-TTG^+G^+... (right-handed) or ...$G^-G^-TTG^-G^-TT$... conformational sequences starting from a fully extended chain. Since this transformation is direct and occurs in a very short time, it necessarily requires that, in a given ordered aggregate of sPP chains initially in form III, gauche bonds having the same sign are formed cooperatively, for steric reasons, as sketched in Figure 13B. The parallelism of the chains may be, indeed, preserved only if the helical stretches, which form from the extended chains, are isochiral, i.e., gauche bonds have all the same sign (G^+ or G^-). In fact, formation of right- and left-handed helical stretches (as in the stable form I) appears sterically forbidden, because it would result in two local stem orientations, which would diverge on opposite sides of the initial trans-planar chain (Figure 13B′) producing steric interactions with the neighboring chains. The two enantiomorphic helical stretches would be oriented at right angle each other. This kind of arrangement has been observed in the γ form of isotactic polypropylene,[39] but it is not feasible for sPP in the crystalline state. As a consequence, during the transformation, helical sequences generated in neighboring chains have the same chirality in order to avoid steric interactions, and the isochiral form II is obtained, even though the antichiral form I is more stable. Thus, the formation of isochiral form II from trans-planar form III, instead of the more stable antichiral form I, in oriented sPP samples, upon releasing the tension, is a fast and cooperative process, governed by rigid steric constraints. The cooperativity of gauche bond formation, indeed, applies to traveling in unison along the extended chains in the whole ordered domain, in a very short time.

It is worth noting that the model of Figure 13B is similar to the structural models including the kink−band disorder proposed to explain some X-ray diffraction and solid-state ^{13}C NMR features observed in low stereoregular sPP samples, crystallized in form II by quench-precipitation from solution[35,36] and in as-prepared samples of syndiotactic copolymers of propylene with ethylene.[40−42] The model of Figure 13B, however, does not represent any intermediate structural model which forms while stretching sPP samples, but it rather

illustrates a possible transient state of the crystalline aggregates of sPP chains, occurring during the crystal−crystal phase transition between form II and form III. In fact, according to the results of the present investigation, the crystal−crystal phase transition between form II and form III of sPP is a fast and direct process, not involving any intermediate phase.

Concluding Remarks

The mechanism of the stress-induced, reversible, crystal−crystal phase transition associated with the elastic behavior of sPP and the time scale of this process has been investigated. The structural changes of unoriented and oriented films of two sPP samples having different stereoregularity have been followed during deformation, by wide-angle X-ray diffraction measurements, using syncrotron radiation.

sPP samples were cyclically stretched and relaxed at controlled rate, while recording X-ray fiber diffraction patterns and stress−strain curves. The results of the present analysis clearly indicate that the structural transition of sPP between form II and form III is a fast and direct process, occurring on the same time scale as the rate the material is strained. During the stretching the transition of the helical form II into the trans-planar form III starts in correspondence of characteristic values of stress−strain parameters. As the strain increases, crystals in form II transform into form III, and the inverse transition occurs, releasing the tension. Below a critical strain, the sample is almost completely in the helical form, as in the initial, unstrained state. A complete recovery of the initial dimension of the specimen is observed, upon releasing the tension. Moreover, the total amount of crystallinity does not change during cyclic elongation and recovery. This suggests that the reversible phase transition between form II and form III does not involve the formation of any disordered, intermediate phase; i.e., it is a direct and cooperative process, implying conformational and structural rearrangements of large bundles of close neighboring chains and occurs instantaneously.

These data indicate that while the driving force leading the conventional elastomers to recover the initial dimensions is merely entropic, in the case of sPP elasticity is also assisted by the enthalpic gain achieved when the sample is relaxed. When the tension is removed, both the enthalpic factor, due to the structural transition in the crystalline region, and an entropic factor, due to the conformational transition of the entangled chains in the amorphous phase, contribute to the elastic recovery of the fiber.

A possible mechanism of the solid−solid martensitic phase transition of sPP is presented. In ref 27, it was argued that the evolution of form III into form II is imposed by conformational and steric constraints and the isochirality of the resulting helical phase was taken as an indication that the transformation is a cooperative process. Our experiments strongly support the cooperativity of this stress-induced phase transition. It thus appears that the generation of the isochiral form II instead of the more stable antichiral form I from the all-trans form III of sPP, upon releasing the tension is a consequence of the cooperative formation of helical stretches having the same chirality, necessary to avoid steric interactions.

Acknowledgment. Financial support from the The "Ministero dell' Istruzione, Università e Ricerca" (PRIN 2002 and Cluster C26) is gratefully acknowledged. We are also thankful to the European Syncrotron Facility (ESRF), Grenoble, France, for X-ray measurements. We also thank Prof. Sanjay Rastogi (Eindhoven University of Technology, Eindhoven, the Netherland) for the useful discussions, Dr. Frank van der Burgt for his help during experiments and Dr. A. Razavi (ATOFINA Petrolchemical Research) for providing the sample.

References and Notes

(1) Ewen, J. A.; Jones, R. L.; Razavi, A.; Ferrara, J. D. *J. Am. Chem. Soc.* **1988**, *110*, 6255.
(2) Lotz, B.; Lovinger, A. J.; Cais, R. E. *Macromolecules* **1988**, *21*, 2375.
(3) Lovinger, A. J.; Lotz, B.; Davis, D. D. *Polymer* **1990**, *31*, 2253.
(4) Lovinger, A. J.; Davis, D. D.; Lotz, B. *Macromolecules* **1991**, *24*, 552.
(5) De Rosa, C.; Corradini, P. *Macromolecules* **1993**, *26*, 5711.
(6) Auriemma, F.; De Rosa, C.; Corradini, P. *Macromolecules* **1993**, *26*, 5719.
(7) Natta, G.; Mazzanti, G.; Crespi, G.; Moraglio, G. *Chim. Ind. (Milano)* **1957**, *39*, 275.
(8) Natta, G. *J. Polym. Sci.* **1959**, *34*, 531.
(9) Natta, G.; Corradini, P.; Ganis, P. *Makromol. Chem.* **1960**, *39*, 238.
(10) Natta, G.; Pasquon, I.; Corradini, P.; Peraldo, M.; Zambelli, A. *Atti Accad. Naz. Lincei, Sci. Fis. Mater. Nat. Rend.* **1960**, *28*, 539.
(11) Zambelli, A.; Locatelli, P.; Provasoli, A.; Ferro, D. R. *Macromolecules* **1980**, *13*, 267.
(12) Ammendola, P.; Shijing, X.; Grassi, A.; Zambelli, A. *Gazz. Chim. Ital.* **1988**, *118*, 769.
(13) De Rosa, C.; Auriemma, F.; Corradini, P. *Macromolecules* **1996**, *29*, 7452.
(14) De Rosa, C.; Auriemma, F.; Vinti, V. *Macromolecules* **1997**, *30*, 4137.
(15) Corradini, P.; Natta, G.; Ganis, P.; Temussi, P. A. *J. Polym. Sci., Part C* **1967**, *16*, 2477.
(16) De Rosa, C.; Auriemma, F.; Vinti, V. *Macromolecules* **1998**, *31*, 7430.
(17) Natta, G.; Peraldo, M.; Allegra, G. *Makromol. Chem.* **1965**, *75*, 215.
(18) Chatani, Y.; Maruyama, H.; Noguchi, K.; Asanuma, T.; Shiomura, T. *J. Polym. Sci., Part C* **1990**, *28*, 393.
(19) Chatani, Y.; Maruyama, H.; Asanuma, T.; Shiomura, T. *J. Polym. Sci., Polym. Lett.* **1990**, *28*, 393.
(20) Auriemma, F.; De Rosa, C.; Ruiz de Ballesteros, O.; Vinti, V.; Corradini, P. *J. Polym. Sci., Polym. Phys.* **1998**, *36*, 395.
(21) Loos, J.; Schimanski, T. *Polym. Eng. Sci.* **2000**, *40*, 567.
(22) D' Aniello, C.; Guadagno, L.; Naddeo, C.; Vittoria, V. *Macromol. Chem. Rapid Commun.* **2001**, *22*, 104.
(23) Auriemma, F.; Ruiz de Ballesteros, O.; De Rosa, C. *Macromolecules* **2001**, *34*, 4485.
(24) Tobolsky, A. V. *Properties and Structure of Polymers*; John Wiley & Sons: New York, 1960.
(25) Treolar, L. R. G. *The Physics of Rubber Elasticity*; Clarendon Press: Oxford, England, 1975.
(26) De Rosa, C.; Gargiulo, M. C.; Auriemma, F.; Ruiz de Ballesteros, O.; Razavi, A. *Macromolecules* **2002**, *35*, 9083.
(27) Lotz, B.; Mathieu, C.; Thierry, A.; Lovinger, A. J.; De Rosa, C.; Ruiz de Ballesteros, O.; Auriemma, F. *Macromolecules* **1998**, *31*, 9253.
(28) Auriemma, F.; De Rosa, C. *J. Am. Chem. Soc.* **2003**, *125*, 13143.
(29) Khachaturyan, A. G. *Theory of Structural Transformations in Solids*; John Wiley & Sons: New York, 1983.
(30) See for instance: Peterlin, A. *Encyclopedia of Polymer Science and Engeneering*; Wiley: New York, 1987; Vol. 10, p 26.
(31) Choi, D.; White, J. L. *Int. Polym. Proc.* **2000**, *15*, 398.
(32) Choi, D.; White, J. L. *Polym. Eng. Sci.* **2001**, *41*, 1743.
(33) Choi, D.; White, J. L. *Polym. Eng. Sci.* **2002**, *42*, 1642.
(34) Palmo, K.; Krimm, S. *Macromolecules* **2002**, *35*, 394.
(35) Auriemma, F.; Born, R.; Spiess, H. W.; De Rosa, C.; Corradini, P. *Macromolecules* **1995**, *28*, 6902.
(36) Auriemma, F.; De Rosa, C.; Ruiz de Ballesteros, O.; Corradini, P. *Macromoleules* **1997**, *30*, 6586.
(37) Rastogi, S.; La Camera, D.; van der Burgt, F.; Terry, A. E.; Cheng, S. Z. D. *Macromolecules* **2001**, *34*, 7730.
(38) De Rosa, C.; Auriemma, F.; Orlando, I.; Talarico, G.; Caporaso, L. *Macromolecules* **2001**, *34*, 1663.
(39) Brückner, S.; Meille, S. V. *Nature (London)* **1989**, *340*, 455.

(40) De Rosa, C.; Auriemma, F.; Vinti, V.; Grassi, A.; Galimberti, M. *Polymer* **1998**, *39*, 6219.
(41) De Rosa, C.; Auriemma, F.; Talarico, G.; Busico, V.; Caporaso, L.; Capitani, D. *Macromolecules* **2002**, *35*, 1314.
(42) De Rosa, C.; Auriemma, F.; Fanelli, E.; Talarico, G.; Capitani, D. *Macromolecules* **2003**, *36*, 1850.

MA0350718